

# THE EVALUATION OF AMERICAN COMPOUND OPTION PRICES UNDER STOCHASTIC VOLATILITY AND STOCHASTIC INTEREST RATES

CARL CHIARELLA<sup>#</sup> AND BODA KANG<sup>†</sup>

ABSTRACT. A compound option (the mother option) gives the holder the right, but not obligation to buy (long) or sell (short) the underlying option (the daughter option). In this paper, we consider the problem of pricing American-type compound options when the underlying dynamics follow Heston's stochastic volatility and with stochastic interest rate driven by Cox-Ingersoll-Ross (CIR) processes. We use a partial differential equation (PDE) approach to obtain a numerical solution. The problem is formulated as the solution to a two-pass free boundary PDE problem which is solved via a sparse grid approach and is found to be accurate and efficient compared with the results from a benchmark solution based on a least-squares Monte Carlo simulation combined with the PSOR.

**Keywords:** American compound option, stochastic volatility, stochastic interest rates, free boundary problem, sparse grid, combination technique, least squares Monte Carlo.

**JEL Classification:** C61, D11.

## 1. INTRODUCTION

The compound option goes back to the seminal paper of Black & Scholes (1973). As well as their famous pricing formulae for vanilla European call and put options, they also considered how to evaluate the equity of a company that has coupon bonds outstanding. They argued that the equity can be viewed as a “compound option” because the equity “is an option on an option on  $\dots$  an option on the firm”. Geske (1979) developed the first closed-form solution for the price of a vanilla European call on a European call. It turns out that a wide variety of important problems are closely related to the valuation of compound options. Some examples include pricing American puts in Geske & Johnson (1984) and hedging volatility risk by trading options on straddles in Brenner, Ou & Zhang (2006).

A compound option (called the mother option) gives the holder the right, but not obligation to buy (long) or sell (short) the underlying option (called the daughter option).

---

<sup>#</sup> carl.chiarella@uts.edu.au; Finance Discipline Group, University of Technology, Sydney, Australia.

<sup>†</sup> Corresponding author: boda.kang@uts.edu.au; Finance Discipline Group, University of Technology, Sydney, PO Box 123, Broadway, NSW 2007, Australia.

For simplicity, we describe the European-type compound option as an example. Suppose that a compound option expires at some date  $T_M$  with the strike price  $K_M$  and the daughter option on which it is contingent, expires at a later time  $T_D (> T_M)$  with the strike price  $K_D$ . Under Geometric Brownian Motion dynamics, the price of a European put on a European put,  $M(S, t)$ , (or put on put for short) may be written as a conditional expectation under the risk neutral measure of the discounted payoff at the maturity of the mother option where the payoff is the positive part of the differences between the price of the daughter option at that time and the strike of the mother option. Similarly, one can define put on call, call on put, and call on call.

Compound options are common in many multi-phase projects, such as product and drug development, where the initiation of one phase of the project depends on the successful completion of the preceding phase. For example, launching a product that involves a new technology requires successful testing of the technology; drug approval is dependent on successful Phase II trials, which can be conducted only after successful Phase I tests. With compound options, at the end of each phase, one has the option to continue to the next phase, abandon the project, or defer it to a later time. Each phase becomes an option that is contingent upon the exercise of earlier options. For phased projects, two or more phases may occur at the same time (parallel options) or in sequence (staged or sequential options). These options are mostly American with the right to buy (call) or sell (put) on or before the expiry of each option. We refer the reader to Kodukula & Papudesu (2006) for more examples of compound options in real option applications.

Derivative securities are commonly written on underlying assets with return dynamics that are not sufficiently well described by the geometric Brownian motion (GBM) process proposed by Black & Scholes (1973). There have been numerous efforts to develop alternative asset return models that are capable of capturing the leptokurtic features found in financial market data, and subsequently to use these models to develop option prices that better reflect the volatility smiles and skews found in market traded options. One of the classical ways to develop option pricing models that are capable of generating such behaviour is to allow the volatility to evolve stochastically, for instance according to the square-root process introduced by Heston (1993). Since we consider the pricing of American-type options, the early exercise premium of the option depends on the cost of carry determined by interest rates. Consequently, the volatility of interest rates does affect the decision to exercise this option at any given point in time. Hence the compound options of the type that we consider in this paper are very sensitive not only to the volatility of the underlying but also to the risk free interest rate, and this is the motivation for considering American-type compound options under stochastic volatility and stochastic interest rates.

Han (2003) in his thesis and Fouque & Han (2005) introduce a fast, efficient and robust approximation to compute the prices of compound options such as call-on-call options within the context of multiscale stochastic volatility models. However, they only consider the case of a European option on a European option. Furthermore their method relies on certain expansions, so its range of validity is not entirely clear.

To the best of our knowledge, there is no literature studying the compound option pricing problem under both stochastic volatility and stochastic interest rates, but some authors do discuss the American option pricing problem under these dynamics. Boyarchenko & Levendorski (2007) formulate the option pricing problem by a PDE approach and they calculate the option prices with the help of an iteration method based on Wiener-Hopf factorization. Medvedev & Scaillet (2010) introduce a new analytical approach. After using an explicit and intuitive proxy for the exercise rule, they derive tractable pricing formulae using a short-maturity asymptotic expansion. Depending on model parameters, this method can accurately price options with time-to-maturity up to several years.

In the case of European options on European options under GBM dynamics, there exist “almost” explicit integral-form solutions. However, in situations involving more general dynamics (such as stochastic volatility), either explicit solutions do not exist or the integrals become difficult to evaluate. In contrast it turns out that the PDE approach provides a very efficient and flexible way to compute prices of compound options. The use of this approach is not restricted to European-type options, and can also include American type, Asian type, or other exotic types of options.

In this paper, we demonstrate the PDE approach to the problem of pricing American-type compound options. We assume that both the mother and the daughter options may be American-type. The American meaning of the mother option is the same as the conventional American option, namely the holder of the compound option can exercise the mother option at any time before the maturity  $T_M$ . Upon exercising the mother option, the holder will hold a daughter option from the early exercise time and we assume that the holder can exercise the daughter option any time from then until the maturity  $T_D$ . In principle, the method we develop is able to price all four kinds of compound options, but here we only give details of the case of an American put on an American put.

The remainder of the paper is structured as follows. Section 2 outlines the problem of an American type compound option where the underlying asset follows stochastic volatility and stochastic interest rate dynamics. In Section 3 we outline the basic idea of the sparse grid approach and implement a combination technique on a sparse grid to find the price profile of a daughter option and apply the same technique to find the price

profile of the mother option based on the results from the previous step. A number of numerical examples that demonstrate the computational advantages of the sparse grid approach are provided in Section 4 before we draw some conclusions in Section 5.

## 2. PROBLEM STATEMENT-COMPOUND OPTION WITH STOCHASTIC VOLATILITY AND STOCHASTIC INTEREST RATES

Let  $D(S, v, r, t)$  denote the price of an American put option (the daughter option) written on a stock of price  $S$  at time  $t$  with maturity time  $T_D$  and strike price  $K_D$  and let  $M(S, v, r, t)$  denote the price of an American put option written on the daughter option of price  $D(S, v, r, t)$  with maturity time  $T_M (< T_D)$  and strike price  $K_M$ . The variables  $v$  and  $r$  denote the variance of the stock price return and the risk free rate at time  $t$ , respectively.

Analogously to the setting in Heston (1993) with in addition a stochastic interest rate of the Cox-Ingersoll-Ross (CIR) type, the dynamics for the share price  $S$  under the risk neutral measure are governed by the stochastic differential equation (SDE) system <sup>1</sup>

$$dS = (r - q)Sdt + \sqrt{v}SdZ_1, \quad (1)$$

$$dv = \kappa_v(\theta_v - v)dt + \sigma_v\sqrt{v}dZ_2, \quad (2)$$

$$dr = \kappa_r(\theta_r - r)dt + \sigma_r\sqrt{r}dZ_3, \quad (3)$$

where  $Z_1, Z_2$  and  $Z_3$  are standard Wiener processes and  $\mathbb{E}(dZ_i dZ_j) = \rho_{ij}dt, i = 1, 2; j = i + 1, \dots, 3$  with  $\mathbb{E}$  being the expectation operator under the risk neutral measure. In (1),  $r$  is the risk free rate of interest and  $q$  is the continuously compounded dividend yield. In (2) the parameter  $\sigma_v$  is the so called vol-of-vol (in fact,  $\sigma_v^2 v$  is the variance of the variance process  $v$ ). The parameters  $\kappa_v$  and  $\theta_v$  are respectively the rate of mean reversion and long run variance of the process for the variance  $v$ . In (3) the parameter  $\sigma_r$  is the volatility of the interest rate process (in fact,  $\sigma_r^2 r$  is the variance of the interest rate process  $r$ ). The parameters  $\kappa_r$  and  $\theta_r$  are respectively the rate of mean reversion and long run interest rate of the process for the interest rate  $r$ .

These parameters are under the risk-neutral measure and are related to the corresponding quantities under the physical measure (that we denote as  $\kappa_v^{\mathbb{P}}, \theta_v^{\mathbb{P}}, \kappa_r^{\mathbb{P}}$  and  $\theta_r^{\mathbb{P}}$ ) by two

---

<sup>1</sup>Of course, since we are using a numerical technique we could in fact use more general processes for  $S$  and  $v$ . The choice of the Heston processes is driven partly by the fact that this has become a very traditional stochastic volatility model and partly because the transform methods (which are used to derive the benchmark prices by the Fourier Cosine Expansion method) do not easily handle the more general variance processes.

parameters that appear in the market prices of both volatility risk and interest rate risk.<sup>2</sup>

We are also able to write down the above system (1)–(3) using independent Wiener processes  $W_1, W_2$  and  $W_3$  so that,

$$\begin{pmatrix} dZ_1 \\ dZ_2 \\ dZ_3 \end{pmatrix} = \begin{pmatrix} 1 & 0 & 0 \\ \rho_{12} & \sqrt{1-\rho_{12}^2} & 0 \\ \rho_{13} & \frac{\rho_{23}-\rho_{13}\rho_{12}}{\sqrt{1-\rho_{12}^2}} & \sqrt{1-\rho_{13}^2 - \left(\frac{\rho_{23}-\rho_{13}\rho_{12}}{\sqrt{1-\rho_{12}^2}}\right)^2} \end{pmatrix} \begin{pmatrix} dW_1 \\ dW_2 \\ dW_3 \end{pmatrix}.$$

The price of an American compound option under stochastic volatility at time  $t$ ,  $M(S, v, r, t)$ , can be formulated as the solution to a two-pass free boundary PDE problem. We first solve the PDE for the value of the daughter option  $D(S, v, r, t)$  given by

$$\mathcal{K}D - rD + \frac{\partial D}{\partial t} = 0, \quad (4)$$

on the interval  $0 \leq t \leq T_D$  and subject to the terminal condition

$$D(S, v, r, T_D) = (K_D - S)^+, \quad (5)$$

and free (early exercise) boundary condition

$$D(d(v, r, t), v, r, t) = K_D - d(v, r, t), \quad (6)$$

and the smooth-pasting conditions

$$\lim_{S \rightarrow d(v, r, t)} \frac{\partial D}{\partial S} = -1, \quad \lim_{S \rightarrow d(v, r, t)} \frac{\partial D}{\partial v} = 0, \quad \lim_{S \rightarrow d(v, r, t)} \frac{\partial D}{\partial r} = 0, \quad (7)$$

where  $S = d(v, r, t)$  is the early exercise boundary for the daughter option at time  $t$ , variance  $v$  and interest rate  $r$ .

In (4) the Kolmogorov operator  $\mathcal{K}$  is given by

$$\begin{aligned} \mathcal{K} = & \frac{vS^2}{2} \frac{\partial^2}{\partial S^2} + \frac{\sigma_v^2 v}{2} \frac{\partial^2}{\partial v^2} + \frac{\sigma_r^2 r}{2} \frac{\partial^2}{\partial r^2} + \rho_{12} \sigma_v v S \frac{\partial^2}{\partial S \partial v} + \rho_{13} \sigma_r r S \frac{\partial^2}{\partial S \partial r} + \rho_{23} \sigma_v \sigma_r v r \frac{\partial^2}{\partial v \partial r} + \\ & (\kappa_r (\theta_r - r) - \lambda_r r) \frac{\partial}{\partial r} + (r - q) S \frac{\partial}{\partial S} + (\kappa_v (\theta_v - v) - \lambda_v v) \frac{\partial}{\partial v}, \end{aligned} \quad (8)$$

<sup>2</sup> In fact, if it is assumed that the market prices of risk associated with the uncertainty driving the variance process and the interest rate process have the form  $\lambda_v \sqrt{v}$  and  $\lambda_r \sqrt{r}$ , respectively, where  $\lambda_v$  is a constant (this was the assumption in Heston (1993)) and  $\lambda_r$  is a constant. In addition  $\kappa_v^{\mathbb{P}}, \theta_v^{\mathbb{P}}$  and  $\kappa_r^{\mathbb{P}}, \theta_r^{\mathbb{P}}$  are the corresponding parameters under the physical measure. Then  $\kappa_v = \kappa_v^{\mathbb{P}} + \lambda_v \sigma_v$ ,  $\theta_v = \frac{\kappa_v^{\mathbb{P}} \theta_v^{\mathbb{P}}}{\kappa_v^{\mathbb{P}} + \lambda_v \sigma_v}$ ;

$\kappa_r = \kappa_r^{\mathbb{P}} + \lambda_r \sigma_r$ ,  $\theta_r = \frac{\kappa_r^{\mathbb{P}} \theta_r^{\mathbb{P}}}{\kappa_r^{\mathbb{P}} + \lambda_r \sigma_r}$ .

where  $\lambda_v$  and  $\lambda_r$  are the constants appearing in the equation for the market prices of volatility risk and interest rate risk, which as stated in Footnote 2 are assumed to be of the form  $\lambda_v\sqrt{v}$  and  $\lambda_r\sqrt{r}$ , respectively.

Given the values for the daughter option, we can then solve the PDE for the mother option  $M(S, v, r, t)$  that satisfies

$$\mathcal{K}M - rM + \frac{\partial M}{\partial t} = 0, \quad (9)$$

on the interval  $0 \leq t \leq T_M$  and subject to the terminal condition

$$M(S, v, r, T_M) = (K_M - D(S, v, r, T_M))^+, \quad (10)$$

the free (early exercise) boundary condition

$$M(m(v, r, t), v, r, t) = K_M - D(m(v, r, t), v, r, t), \quad (11)$$

and the smooth-pasting conditions

$$\lim_{S \rightarrow m(v, r, t)} \frac{\partial M}{\partial S} = -\frac{\partial D}{\partial S}, \quad \lim_{S \rightarrow m(v, r, t)} \frac{\partial M}{\partial v} = -\frac{\partial D}{\partial v}, \quad \lim_{S \rightarrow m(v, r, t)} \frac{\partial M}{\partial r} = -\frac{\partial D}{\partial r}, \quad (12)$$

where  $m(v, r, t)$  is the early exercise boundary for the mother option at variance  $v$ , interest rate  $r$  and time  $t$ .

### 3. SPARSE GRID IMPLEMENTATION

In order to tackle the computationally demanding task of solving the two nested PDEs (4)–(6) and (9)–(11) we apply the sparse grid approach that turns out to be quite fast and accurate. The sparse grid *combination technique* for solving PDEs was first introduced by Griebel, Schneider & Zenger (1992) after which Reisinger (2004) in his PhD thesis, Reisinger & Wittum (2007), Leentvaar & Oosterlee (2008a) and Leentvaar & Oosterlee (2008b) discussed the application of this approach to various option pricing problems. The combination technique requires the solution of the original equation only on a set of conventional subspaces defined on Cartesian grids specified in a certain way and a subsequent extrapolation step, but still retains a certain order convergence.

In fact we can identify three desirable properties of the combined solution. First of all, in comparison to the standard full grid approach the number of grid points can be reduced significantly from  $O(2^{n \cdot d})$  to  $O(2^n \cdot n^{d-1})$  at refinement level  $n$  in the  $d$ -dimensional case, whereas the point-wise accuracy of the approximation to the solution of the PDE is  $O(n^{d-1} \cdot 2^{-n \cdot p})$  which is only slightly worse than  $O(2^{-n \cdot p})$ . Here,  $p$  includes the order of the underlying discretization scheme, as well as the influence of singularities. Furthermore, each of the Cartesian grids setting up the sparse grid only consists of  $O(2^n)$

nodes. Thus, the efficient usage of sparse grids for the computational solution of the PDE greatly reduces storage requirements and computing time at a moderate cost of accuracy.

Secondly, we have to point out the simplicity of the combination concept: we have seen that the sparse grid combined solution represents a linear combination of numerical solutions on Cartesian grids corresponding to the components of a sparse grid at the same refinement level. Thus, the combination technique allows for the integration of existing solvers for partial differential equations on traditional full grids. In contrast to the discretization on a real sparse grid, which requires hierarchical data structures and thus specially designed solvers, the combined solution is built on simple data structures and can be based on any “black box solver”. Only the final linear combination of these simple solutions has to be newly implemented.

From the combined solution as a linear combination of traditional full grid discretizations we can also deduce a further advantage of the combination technique. Since the  $O(n^{d-1})$  problems solved on the Cartesian grids  $\Omega_l$  that set up the sparse grids are independent from one another, these problems can be solved in parallel on different workstations. Communication has to take place only at the end, where the summation and the extrapolation by linear combination of the different solutions is performed.

**3.1. The Sparse grid combination technique.** We incorporate the techniques and algorithms used in Chiarella, Ziogas & Ziveyi (2010) and the sparse grid approach to solve the linked PDEs (4)–(6) and (9)–(11) with suitable initial, boundary conditions.

In a general  $d$ -dimensional unit cube and the family of grids with grid sizes  $h_j = 2^{-l_j}$  in direction  $j$ ,  $l_j \in \mathbb{N}_0$ . We write the vector of grid sizes as  $\mathbf{h} = 2^{-\mathbf{l}}$  with  $\mathbf{l} = (l_1, \dots, l_d) \in \mathbb{N}_0^d$  and denote the solution of the PDE on those grids by  $p_{\mathbf{h}}$ . The sparse grid solution at level  $l$  is then defined as

$$p_l = \sum_{k=l}^{l+d-1} a_{l-k} \sum_{l_1+\dots+l_d=k} p_{\mathbf{h}}, \quad (13)$$

with

$$a_k = (-1)^{d-1-k} \binom{d-1}{k}, \quad 0 \leq k \leq d-1. \quad (14)$$

In our case  $d = 3$  hence we consider a truncated 3-dimensional cube  $\Omega := [0, S_{\max}] \times [0, v_{\max}] \times [0, r_{\max}]$  and a Cartesian grid with mesh size  $h_j = 2^{-l_j}$  (corresponding to a level  $l_j \in \mathbb{N}_0$ ) in the directions  $j = 1, 2, 3$ . The indices  $j = 1$ ,  $j = 2$  and  $j = 3$  represent the directions of the stock price  $S$ , the variance  $v$  and the interest rate  $r$  respectively.

For a vector  $\mathbf{h} = (h_1, h_2, h_3)$  we denote by  $p_{\mathbf{h}}$  the representation of a function on such a grid with points

$$\mathbf{x}_h = (i_1 \cdot h_1, i_2 \cdot h_2, i_3 \cdot h_3), \quad 1 \leq i_j \leq N_j, \quad N_j = 1/h_j = 2^{l_j}, \quad \text{for } j = 1, 2, 3.$$

For a given level  $l$ , the above grid consists all possible combinations of  $(l_1, l_2, l_3)$  with  $0 \leq l_1, l_2, l_3 \leq l$ . Hence, in total, there are  $(2^l + 1)^3$  points in the grid. The number of total points in the full grid increases significantly with the increase of the level  $l$ . It will be quite expensive to solve the two-pass PDE system on the above full grid.

However, with the same level  $l$ , the *sparse* grid, will consist of the following points

$$\mathbf{x}_h = (i_1 \cdot h_1, i_2 \cdot h_2, i_3 \cdot h_3), \quad 1 \leq i_j \leq N_j, \quad N_j = 1/h_j = c_j 2^{l_j}, \quad \text{for } j = 1, 2, 3.$$

satisfying  $l_1 + l_2 + l_3 = l$  and where  $c_j$  are some positive constants with the help of which it is possible to construct a non-equidistant grid.

It is not hard to see that there are  $\binom{l+d-1}{d-1}$  choices of such combinations of  $(l_1, l_2, l_3)$  such that  $l_1 + l_2 + l_3 = l$ . Figures 1–3 provide an example of a standard sparse grid hierarchy with level  $l = 3, l = 2$  and  $l = 1$  with respect to 10, 6 and 3 different combinations corresponding to each level respectively.

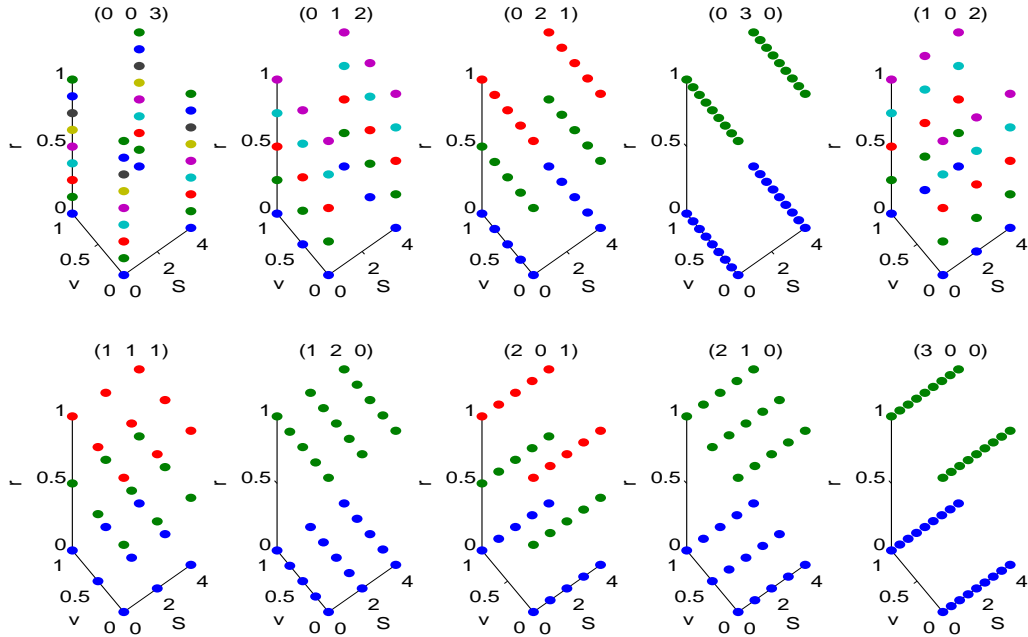


FIGURE 1. A sparse grid hierarchy of level 3 with respect to each combination. From the left to right and from top to bottom, these are  $(0, 0, 3), (0, 1, 2), \dots, (2, 1, 0), (3, 0, 0)$  respectively.



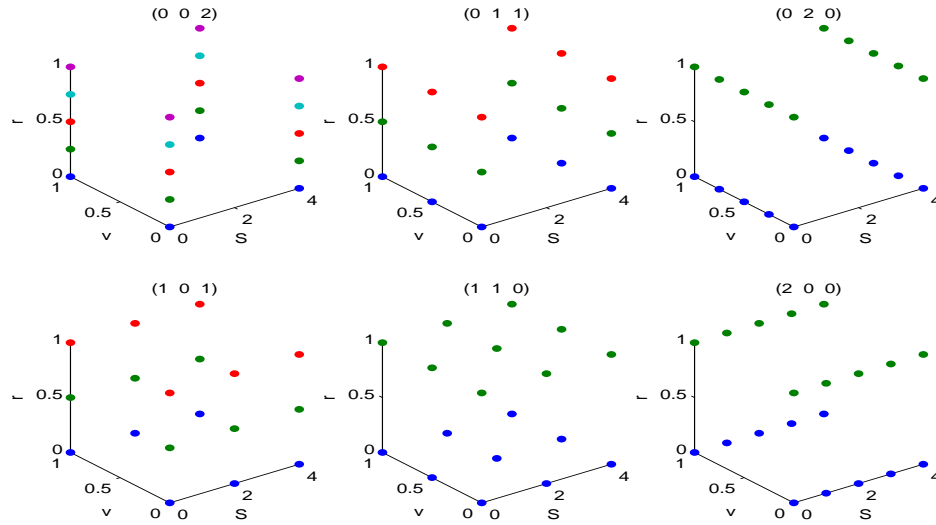


FIGURE 2. A sparse grid hierarchy of level 2 with respect to each combination. From the left to right and from top to bottom, these are  $(0, 0, 2), (0, 1, 1), \dots, (1, 1, 0), (2, 0, 0)$  respectively.

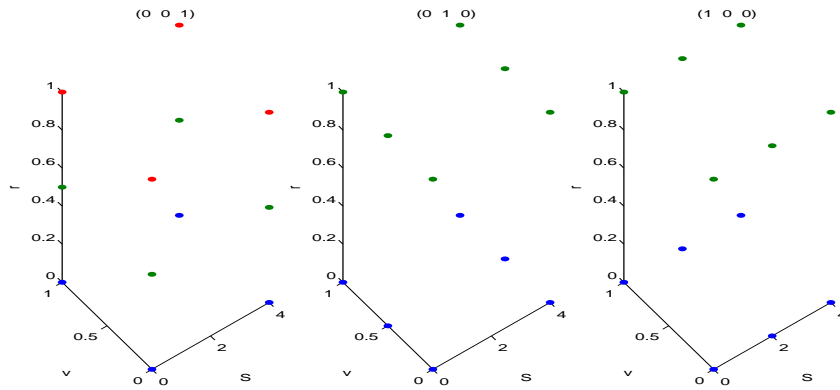


FIGURE 3. A sparse grid hierarchy of level 1 with respect to each combination. From the left to right, these are  $(0, 0, 1), (0, 1, 0), (1, 0, 0)$  respectively.

Obviously, the above grids share the common property that they are dense in one direction but sparse in the other directions. If we put all of the above grids together, we will obtain the standard sparse grid shown in Figure 4.

Let  $\mathbf{p}_h$  be the discrete vector of function values at the grid points of the standard sparse grid. In general,  $\mathbf{p}_h$  is the finite difference solution to the PDE of interest on the corresponding grid  $\mathbf{h}$ . The solution can be extended to  $\Omega$  by a suitable multi-linear

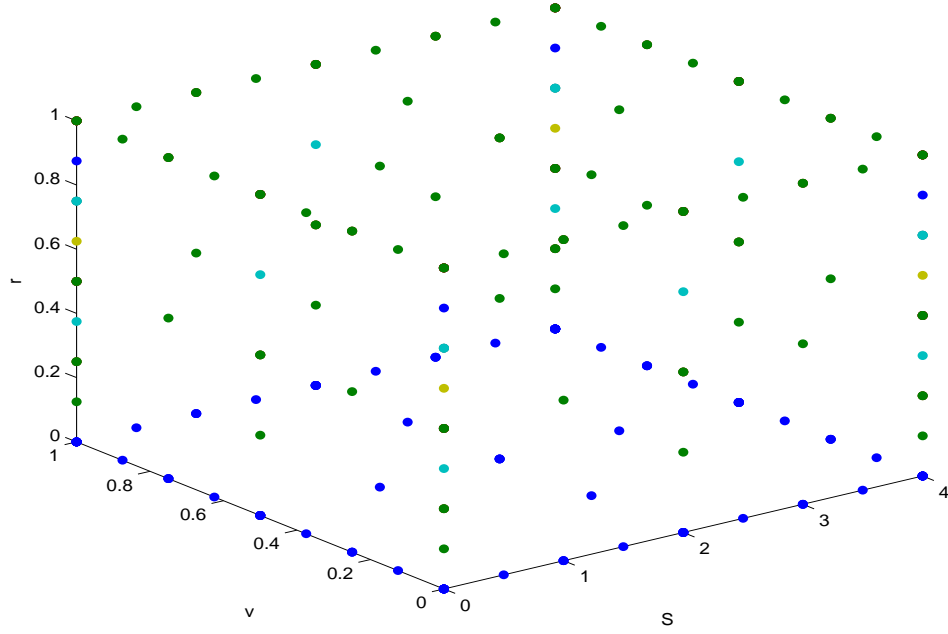


FIGURE 4. A combined sparse grid solution.

interpolation operator  $\mathcal{I}^3$  in the point wise sense according to

$$p_{\mathbf{h}}(S, v, r, \tau) = \mathcal{I}p_{\mathbf{h}}, \forall (S, v, r) \in \Omega.$$

Next, we define the family  $P$  of solutions corresponding to the different sparse grids (as in Figure 1 for instance) by  $P = (P(\mathbf{i}))_{\mathbf{i} \in \mathbb{N}^3}$  with

$$P(\mathbf{i}) := p_{2^{-\mathbf{i}}},$$

that is the family of numerical approximations (after proper interpolation)  $p_{\mathbf{h}}$  on tensor product grids with  $h_k = 2^{-i_k}$ . For example, the solution on the first grid in Figure 1 would be  $P(0, 0, 3)$  etc. The combination technique in Reisinger & Wittum (2007) tells us that the solution  $p_l$  ( $l$  is the level of the sparse grid) of the corresponding PDE is

$$p_l = \sum_{l_1+l_2+l_3=l} P(l_1, l_2, l_3) - 2 \cdot \sum_{l_1+l_2+l_3=l+1} P(l_1, l_2, l_3) + \sum_{l_1+l_2+l_3=l+2} P(l_1, l_2, l_3). \quad (15)$$

The above is a special case of Eqn.(13) and Eqn.(14) when  $d = 3$ .

The procedure involves solving the PDE in parallel on each of the sparse grids of level  $l, l + 1$  and level  $l + 2$  respectively. See Figures 1–3 for  $l = 1$  and  $d = 3$  as an example.

---

<sup>3</sup>A thorough error analysis of the multi-linear interpolation operator can be found in Reisinger (2008) who gives a generic derivation for linear difference schemes through an error correction technique employing semi-discretisations and obtains error formulae as well.

Thus we have

$$\sum_{k=l}^{l+2} \binom{k+d-1}{d-1} = \sum_{k=1}^3 \binom{k+2}{2} = 3 + 6 + 10 = 19$$

which means that there will be 19 PDE solvers running simultaneously when  $l = 1$ . The theory developed by Reisinger & Wittum (2007) shows that Equation (15) combines all solutions together to yield a more accurate solution to the PDE.

The essential principle of the extrapolation is that all lower order error terms cancel out in the combination formula (15) and only the highest order terms

$$h_1^2 \cdot h_2^2 \cdot h_3^2 = (2^{-l_1} \cdot 2^{-l_2} \cdot 2^{-l_3})^2 = 4^{-l}$$

remain. Taking advantage of this cancelation mechanism, Eqn.(15) is able to produce quite accurate results fairly quickly. The details of the error analysis can be found in Reisinger (2004) and Reisinger & Wittum (2007)<sup>4</sup>.

We implement the above sparse grid combination technique to solve the PDE (4) in order to obtain the desired daughter option prices. We thus have the terminal and boundary conditions for the PDE governing the price of the mother option. Next, we apply the technique again to solve the PDE (9) to obtain the prices of the mother option. We solve the PDEs (4)–(6) and (9)–(11) in each of the subspaces on a parallel cluster, which makes the process very efficient.

**3.2. Finite Difference Method with PSOR.** In the implementation, a standard Crank Nicolson finite difference method with the projected successive over-relaxation (PSOR) method has been applied to each of the sparse grids in Figures 1–3 to work out the solution of both PDEs (4)–(6) and (9)–(11) on the grid points, solutions at other non-grid points are obtained by the same multi-linear interpolation as in Reisinger (2008). The implementation of PSOR is detailed in this section. As an example, we show the detail of solving the PDE followed by the daughter option prices. We apply the same approach to the PDE followed by prices of the mother option with different terminal and boundary conditions. The boundary conditions for the mother option are quite similar to those for daughter options, hence for brevity, we only mention boundary conditions for the daughter option.

---

<sup>4</sup> The combination method requires, theoretically, smoothness of mixed derivatives of the solution. This is obviously not the case here due to the non-smooth payoff. However, if the payoff is aligned with the grid, which is the case in our problem, then good results have been observed for the combination method (see Leentvaar & Oosterlee (2008b)). This is probably due to the rapid smoothing of the payoff in the first few time steps.

It is convenient to consider the time-to-maturity  $\tau = T - t$  instead of time  $t$ . The three space variables  $S, v, r$  and time-to-maturity  $\tau$  are discretised according to,

$$S_i = (i - 1) \cdot \Delta S, \quad i = 1, \dots, N_1 + 1; \quad v_j = (j - 1) \cdot \Delta v, \quad j = 1, \dots, N_2 + 1; \quad (16)$$

$$r_k = (k - 1) \cdot \Delta r, \quad k = 1, \dots, N_3 + 1; \quad \tau_l = T - l\Delta t, \quad l = 1, \dots, N_\tau, \quad (17)$$

with  $N_1, N_2, N_3$  and  $N_\tau$  are the number of grid points in the direction  $S, v, r$  and  $\tau$  respectively.

The option prices at the discrete points thus are

$$D_{i,j,k}^l = D(S_i, v_j, r_k, \tau_l).$$

Similar to the discussions in Ekstrom, Lotstedt & Tysk (2009), we use central differences to approximate most of the first and second derivatives in the PDE but use the forward and backward finite difference approximations on the boundaries other than the time derivative in Eqn. (4). Thus we set,

$$\begin{aligned} \frac{\partial D}{\partial S} &= \frac{D_{i+1,j,k}^l - D_{i-1,j,k}^l}{2\Delta S}, & \frac{\partial^2 D}{\partial S^2} &= \frac{D_{i+1,j,k}^l - 2D_{i,j,k}^l + D_{i-1,j,k}^l}{\Delta S^2}, \\ \frac{\partial D}{\partial v} &= \frac{D_{i,j+1,k}^l - D_{i,j-1,k}^l}{2\Delta v}, & \frac{\partial^2 D}{\partial v^2} &= \frac{D_{i,j+1,k}^l - 2D_{i,j,k}^l + D_{i,j-1,k}^l}{\Delta v^2}, \\ \frac{\partial D}{\partial r} &= \frac{D_{i,j,k+1}^l - D_{i,j,k-1}^l}{2\Delta r}, & \frac{\partial^2 D}{\partial r^2} &= \frac{D_{i,j,k+1}^l - 2D_{i,j,k}^l + D_{i,j,k-1}^l}{\Delta r^2}, \end{aligned}$$

and

$$\begin{aligned} \frac{\partial D}{\partial S} \Big|_{S=S_1} &= \frac{D_{1,j,k}^l - D_{0,j,k}^l}{\Delta S}, & \frac{\partial D}{\partial S} \Big|_{S=S_{N_1}} &= \frac{D_{N_1,j,k}^l - D_{N_1-1,j,k}^l}{\Delta S}, \\ \frac{\partial D}{\partial v} \Big|_{v=v_1} &= \frac{D_{i,1,k}^l - D_{i,0,k}^l}{\Delta v}, & \frac{\partial D}{\partial v} \Big|_{v=v_{N_2}} &= \frac{D_{i,N_2,k}^l - D_{i,N_2-1,k}^l}{\Delta v}, \\ \frac{\partial D}{\partial r} \Big|_{r=r_1} &= \frac{D_{i,j,1}^l - D_{i,j,0}^l}{\Delta r}, & \frac{\partial D}{\partial r} \Big|_{r=r_{N_3}} &= \frac{D_{i,j,N_3}^l - D_{i,j,N_3-1}^l}{\Delta r}. \end{aligned}$$

Similar to Boyarchenko & Levendorski (2007), we use the boundary conditions  $\frac{\partial^2 D}{\partial v^2} = 0$  at the boundaries  $v = 0$  and  $v = v_{\max}$  and boundary conditions  $\frac{\partial^2 D}{\partial r^2} = 0$  at the boundaries  $r = 0$  and  $r = r_{\max}$ . The discretized analogues  $\forall i = 1, \dots, N_1 + 1$  are

$$D_{i,1,k}^l = 2 \cdot D_{i,2,k}^l - D_{i,3,k}^l, \quad D_{i,N_2+1,k}^l = 2 \cdot D_{i,N_2,k}^l - D_{i,N_2-1,k}^l, \quad \forall k = 1, \dots, N_3 + 1;$$

$$D_{i,j,1}^l = 2 \cdot D_{i,j,2}^l - D_{i,j,3}^l, \quad D_{i,j,N_3+1}^l = 2 \cdot D_{i,j,N_3}^l - D_{i,j,N_3-1}^l, \quad \forall j = 1, \dots, N_2 + 1,$$

which is essentially an extrapolation scheme.

All other derivative terms in the  $v, r$ - direction vanish at  $v = 0$  or  $r = 0$  due to the factor  $v, r$  occurring in Equation (4), and hence, these terms do not require further treatment.

We follow Ikonen & Toivanen (2007) to indicate which grid point values we use to approximate the second-order mixed-derivative in order to obtain non positive off-diagonal weights in the finite difference stencil, which makes the matrix an  $M$ -matrix as much as possible.

In fact, to simplify the algorithm and take consideration of the correlations  $\rho_{ij}$ , in each two dimensional space, we use a seven points stencil and the mixed derivatives when  $\rho_{12} > 0$  are approximated as,

$$\frac{\partial D^2}{\partial S \partial v} \approx \frac{1}{2} \left( \frac{D_{i+1,j+1,k}^l - D_{i,j+1,k}^l - (D_{i+1,j,k}^l - D_{i,j,k}^l)}{\Delta S \Delta v} + \frac{D_{i,j,k}^l - D_{i-1,j,k}^l - (D_{i,j-1,k}^l - D_{i-1,j-1,k}^l)}{\Delta S \Delta v} \right)$$

and when  $\rho_{12} < 0$  we have

$$\frac{\partial D^2}{\partial S \partial v} \approx \frac{1}{2} \left( \frac{D_{i,j+1,k}^l - D_{i-1,j+1,k}^l - (D_{i,j,k}^l - D_{i-1,j,k}^l)}{\Delta S \Delta v} + \frac{D_{i+1,j,k}^l - D_{i,j,k}^l - (D_{i+1,j-1,k}^l - D_{i,j-1,k}^l)}{\Delta S \Delta v} \right).$$

The other mixed derivatives  $\frac{\partial^2}{\partial S \partial r}$  and  $\frac{\partial^2}{\partial v \partial r}$  are handled in a similar way depending on the sign of the corresponding correlations.

Boundary conditions at the boundaries  $S = 0$  and  $S = S_{\max}$  for a put option are

$$D_{1,j,k}^l = K_D \cdot e^{-(k-1) \cdot \Delta r \cdot \tau_l}, \quad D_{N_1+1,j,k}^l = 0, \quad \forall j = 1, \dots, N_2 + 1, k = 1, \dots, N_3 + 1;$$

while those are for a call option would be set as:

$$D_{1,j,k}^l = 0, \quad D_{N_1+1,j,k}^l = S_{\max} - K_D \cdot e^{-(k-1) \cdot \Delta r \cdot \tau_l}, \quad \forall j = 1, \dots, N_2 + 1, k = 1, \dots, N_3 + 1;$$

The spatial discretisation above leads to a semi-discrete equation which has the matrix representation

$$\frac{\partial \mathbf{D}}{\partial \tau} + \mathbf{A} \mathbf{D} = 0 \tag{18}$$

where  $\mathbf{A}$  is a block tridiagonal  $(N_1 + 1)(N_2 + 1)(N_3 + 1) \times (N_1 + 1)(N_2 + 1)(N_3 + 1)$  matrix and  $\mathbf{D}$  is a vector of length  $(N_1 + 1)(N_2 + 1)(N_3 + 1)$ .

Next, we implement a more general  $\theta$ -scheme which includes the implicit ( $\theta = 1$ ), the Crank-Nicolson ( $\theta = \frac{1}{2}$ ) and the explicit ( $\theta = 0$ ) approaches to discretise the semi-discrete problem (18) as

$$(\mathbf{I} + \theta \Delta \tau \mathbf{A}) \mathbf{D}^{(l+1)} = (\mathbf{I} - (1 - \theta) \Delta \tau \mathbf{A}) \mathbf{D}^{(l)}, \quad l = 0, \dots, N_\tau - 1, \tag{19}$$

where  $N_\tau$  is the number of time steps and  $\mathbf{I}$  is the identity matrix.

After the discretisation of the underlying PDE with three spatial variables an approximate price of an American option can be obtained by solving a sequence of linear complementarity problems (LCPs)

$$\begin{cases} \mathbf{B}\mathbf{D}^{(l+1)} \geq \mathbf{E}\mathbf{D}^{(l)}, & \mathbf{D}^{(l+1)} \geq \mathbf{g}, \\ \left(\mathbf{B}\mathbf{D}^{(l+1)} - \mathbf{E}\mathbf{D}^{(l)}\right)^T \left(\mathbf{D}^{(l+1)} - \mathbf{g}\right) = 0, \end{cases} \quad (20)$$

for  $l = 0, \dots, N_\tau - 1$ . The matrices  $\mathbf{B}$  and  $\mathbf{E}$  in (20) are defined by the left hand side and right hand side of Eqn. (19) respectively. The initial value  $\mathbf{D}^{(0)}$  is given by the discrete form  $\mathbf{g}$  of the payoff function  $g$  of the option, so that the  $i$ th element of  $\mathbf{D}^{(0)}$  is given by

$$D_i^{(0)} = \max(K - S_i, 0). \quad (21)$$

In order to avoid the oscillations that often occur with the CN scheme, we use the implicit Euler scheme ( $\theta = 1$ ) for the first 3 time steps and then switch to the CN scheme ( $\theta = \frac{1}{2}$ ) in the rest of the time steps. We implemented a PSOR finite difference scheme to solve the sequence (20) of LCPs efficiently.

In order to accelerate the convergence of the PSOR, we need to select the over-relaxation parameter  $\omega$  in the algorithm (see Section 6.2.3 in Kwok (2008)). We notice that we may not choose the same  $\omega$  when we apply PSOR to different discretized grids in Figure 1. Table 2 in the next section demonstrates how the optimal  $\omega$  should be chosen for different grids on a specific numerical example.

#### 4. NUMERICAL EXAMPLES

To demonstrate the performance of the sparse grid algorithm outlined in Section 3 we implement the method for a given set of parameter values. Those parameters are the same as one set of parameters used in Medvedev & Scaillet (2010) for comparison purpose<sup>5</sup>. The parameter values used are listed in Table 1.

In Section 3.2, we mentioned that the over-relaxation parameter  $\omega$  is important to the convergence of the sparse grid approach and it usually depends on the shape of the grids as well. Table 2 illustrates this dependence in the case when  $l = 6$ . It can be seen from the table that the parameter  $\omega$  is usually higher for relatively less balanced grids, such as, (0, 0, 6), (0, 6, 0) etc, in which the calculation will take more time as well.

---

<sup>5</sup>The source code for all methods was implemented using NAG Fortran with the IMSL library running on the UTS, Faculty of Business F&E HPC Linux Cluster which consists of 8 nodes running Red Hat Enterprise Linux 4.0 (64bit) with  $2 \times 3.33$  GHz,  $2 \times 6$  MB cache Quad Core Xeon X5470 Processors with 1333MHz FSB 8GB DDR2-667 RAM.

Option Parameter	Value	SV Parameter	Value	SI Parameters	Value
$q$	0.0	$\theta_v$	0.02	$\theta_r$	0.04
$T_D$	1.0	$\kappa_v$	1.5	$\kappa_r$	0.3
$K_D$	100	$\sigma_v$	0.15	$\sigma_r$	0.1
$T_M$	0.50	$\lambda_v$	0.00	$\lambda_r$	0.00
$K_M$	4	$\rho_{12}$	-0.50	$\rho_{13}, \rho_{23}$	0.0

TABLE 1. Parameter values used for the American put daughter option. The stochastic volatility (SV) and stochastic interest rate (SI) parameters are those used in Medvedev & Scaillet (2010) to facilitate comparisons.

$(l_1, l_2, l_3)$	$\omega$	$(l_1, l_2, l_3)$	$\omega$	$(l_1, l_2, l_3)$	$\omega$	$(l_1, l_2, l_3)$	$\omega$	$(l_1, l_2, l_3)$	$\omega$
(0, 0, 6)	1.6	(0, 1, 5)	1.3	(0, 2, 4)	1.1	(0, 3, 3)	1.1	(0, 4, 2)	1.3
(0, 5, 1)	1.6	(0, 6, 0)	1.8	(1, 0, 5)	1.3	(1, 1, 4)	1.1	(1, 2, 3)	1.1
(1, 3, 2)	1.1	(1, 4, 1)	1.3	(1, 5, 0)	1.6	(2, 0, 4)	1.1	(2, 1, 3)	1.1
(2, 2, 2)	1.1	(2, 3, 1)	1.1	(2, 4, 0)	1.3	(3, 0, 3)	1.1	(3, 1, 2)	1.1
(3, 2, 1)	1.1	(3, 3, 0)	1.1	(4, 0, 2)	1.2	(4, 1, 1)	1.2	(4, 2, 0)	1.2
(5, 0, 1)	1.4	(5, 1, 0)	1.4	(6, 0, 0)	1.7				

TABLE 2. Values of  $\omega$  for different sparse grid are used for the American put daughter option when  $l = 6$ .

In order to compare the option prices with Medvedev & Scaillet (2010) as well as demonstrate the efficiency and accuracy of our sparse grid approach, we first work out European put option prices by implementing the SG approach and compare them with the solution from Grzelak & Oosterlee (2011) using the Fourier Cosine expansion (COS) approach. Table 3 reports the numerical results and Figure 5 demonstrates the rate of the convergence of our SG approach with the increase of the level  $l$ . Table 3 has the following columns:  $l$  defines the level of the sparse grid; the put prices when the spot price goes from 80 to 120; the error column gives the root mean square relative differences (RMSRD<sup>6</sup>) compared with the COS method and the last column gives the runtime of our approach.

Using the level 6 prices in Table 3 as suitable terminal and boundary conditions for the mother options, we are able to work out the prices of the Mother put option on the daughter option. Since we don't have a closed form solution for the mother option, we compare our mother prices against the prices from Monte Carlo simulation using the daughter prices calculated from the COS method. The comparisons are displayed in Table 4<sup>7</sup>.

<sup>6</sup>RMSRD is calculated as:  $\sqrt{\frac{1}{5} \sum_{i=1}^5 \left( \frac{\hat{P}(S_i) - P(S_i)}{P(S_i)} \right)^2}$ , where  $S_i = 80 + 10 \cdot (i - 1)$ ,  $\hat{P}(S)$  is the estimate of the price, and  $P(S)$  is the true price in the last row of Table 3.

<sup>7</sup>Note there is a negative price when  $S = 80, l = 1$ . This is partly because according to Eqn (14), the sequence of the weights are positive and negative interchangeably, for instance, if  $d = 3$ , we have

Level	$S$					RMSRD	Runtime
$l$	80	90	100	110	120		(sec)
1	17.0446	9.7664	4.9921	2.3992	1.1530	$1.56 \times 10^{-2}$	1.31
2	16.9834	9.6920	4.9852	2.4424	1.1738	$5.11 \times 10^{-3}$	4.30
3	16.9640	9.6821	5.0100	2.4612	1.1796	$1.47 \times 10^{-3}$	15.84
4	16.9550	9.6828	5.0210	2.4625	1.1779	$3.22 \times 10^{-4}$	72.97
5	16.9520	9.6849	5.0226	2.4616	1.1774	$4.61 \times 10^{-5}$	329.12
6	16.9514	9.6855	5.0225	2.4616	1.1773	$4.05 \times 10^{-5}$	1517.34
COS	16.9512	9.6856	5.0227	2.4618	1.1774		

TABLE 3. Daughter prices (**European** put) computed using the sparse grid (SG) with  $(c_1 = 16, c_2 = 8, c_3 = 4)$ , Fourier Cosine Expansion Approach. Parameter values are given in Table 1, with  $v_0 = 0.04$  and  $r_0 = 0.04$ .

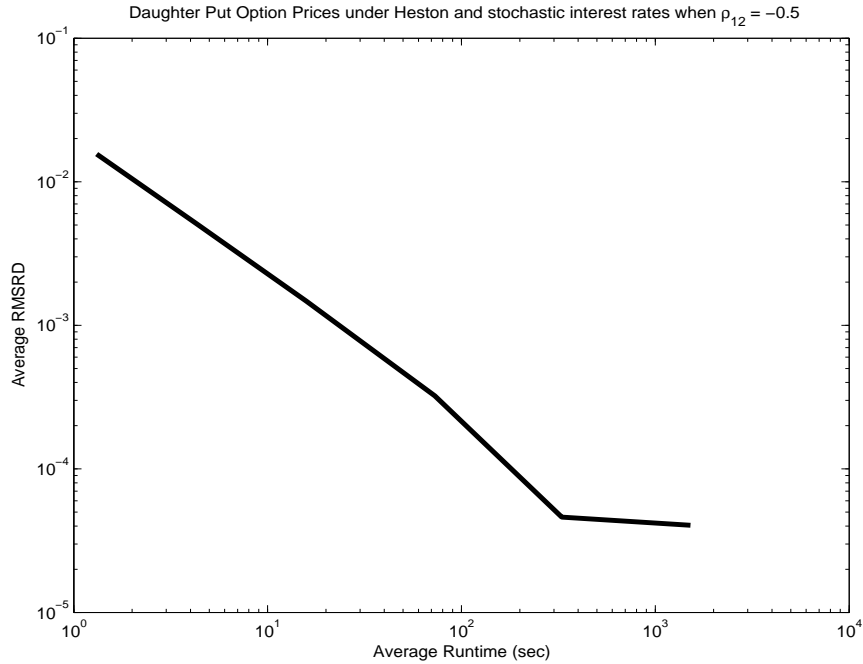


FIGURE 5. Efficiency plot of the prices of the daughter European put option prices under SV and SI model.

We see from the values given in Table 4 that the compound option prices from the sparse grid all lie between the lower and upper bound of the MC simulation approach<sup>8</sup>. However it should be emphasized that the runtime of the sparse grid approach involves the calculations of all compound option prices within the grid whereas the runtime of

$a_0 = 1, a_1 = -2, a_2 = 1$ . Hence, it is possible to produce negative prices especially when the grid is very coarse. However the “combination” technique ensure convergence when the grid becomes finer.

<sup>8</sup>The RMSRD in Tables 4 and 6 are only used to indicate that the results from the sparse grid “converge” in a correct direction.



Level $l$	$S$					RMSRD	Runtime (sec)
	80	90	100	110	120		
1	-0.0326	0.2837	1.2164	2.3713	3.0846	$2.10 \times 10^{-1}$	1.83
2	0.2190	0.8083	1.7392	2.5594	3.1422	$1.55 \times 10^{-1}$	3.48
3	0.1012	0.5743	1.4898	2.4287	3.0852	$2.07 \times 10^{-2}$	12.17
4	0.0724	0.5619	1.4910	2.4144	3.0777	$2.96 \times 10^{-2}$	51.06
5	0.1064	0.6105	1.5229	2.4341	3.0867	$2.50 \times 10^{-2}$	220.37
6	0.1030	0.6052	1.5196	2.4322	3.0861	$1.88 \times 10^{-3}$	820.16
MC+COS	0.1032	0.6079	1.5228	2.4339	3.0889		2388.97
MC Upper Bound	0.1053	0.6129	1.5295	2.4405	3.0942		
MC Lower Bound	0.1011	0.6030	1.5161	2.4273	3.0835		

TABLE 4. Mother prices (**European** put on **European** put) computed using the sparse grid (SG) with  $(c_1 = 16, c_2 = 8, c_3 = 4)$ , Monte Carlo with the Fourier Cosine Expansion Approach. There are 1,000,000 sample paths and 200 time steps in the MC simulation. Parameter values are given in Table 1, with  $v_0 = 0.04$  and  $r_0 = 0.04$ .

the simulation approach is just that required to work out the five prices at the five stock price values given in Table 4. It is clear that the sparse grid approach attains the same accuracy in far less time compared to the simulation approach.

Level $l$	$S$					RMSRD	Runtime (sec)
	80	90	100	110	120		
1	19.3227	10.0150	4.9658	2.4678	1.2260	$6.62 \times 10^{-2}$	1.34
2	20.0596	10.6755	5.2288	2.4966	1.1889	$3.80 \times 10^{-2}$	4.15
3	20.0275	11.0899	5.5819	2.7110	1.2712	$2.01 \times 10^{-2}$	18.33
4	20.0025	11.1125	5.5018	2.6028	1.2264	$8.36 \times 10^{-3}$	79.08
5	20.0232	11.0393	5.4922	2.6377	1.2432	$3.21 \times 10^{-3}$	383.10
6	20.0067	10.9663	5.4969	2.6299	1.2385	$8.85 \times 10^{-4}$	1708.86
PSOR	19.9987	10.9820	5.4899	2.6295	1.2388		124875.00

TABLE 5. Daughter prices (**American** put) computed using the sparse grid (SG) with  $(c_1 = 16, c_2 = 8, c_3 = 4)$ , PSOR in a fine grid. Parameter values are given in Table 1, with  $v_0 = 0.04$  and  $r_0 = 0.04$ .

Table 5 and Figure 6 demonstrate the convergence property of the sparse grid approach calculating the American put option prices under Heston with stochastic interest rate. A finite difference approach with PSOR with a fine grids discretization ( $N_1 = 1024, N_2 = 512, N_3 = 512, N_t = 128$ ) are treated as the benchmark prices. It is clear that the convergence of the sparse grid approach is quite fast.

Since the mother option can be exercised any time prior to the maturity of the compound option, at each time before maturity, in order to make the decisions on the early

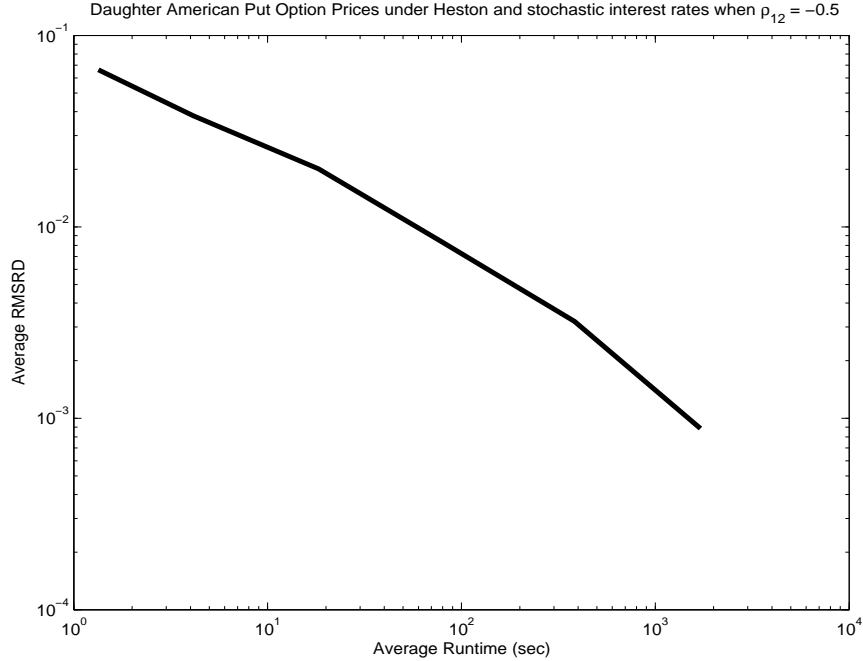


FIGURE 6. Efficiency plot of the prices of the daughter American put option prices under SV and SI model.

Level	$S$					RMSRD	Runtime
$l$	80	90	100	110	120		(sec)
1	0.0487	0.4439	1.3844	2.4962	3.2094	$2.78 \times 10^{-1}$	2.32
2	0.1241	0.6260	1.6071	2.5854	3.2090	$7.33 \times 10^{-2}$	4.38
3	0.0773	0.5538	1.5204	2.4944	3.1782	$1.33 \times 10^{-1}$	14.07
4	0.0924	0.5902	1.5482	2.5080	3.1835	$6.41 \times 10^{-2}$	61.42
5	0.1021	0.6168	1.5721	2.5179	3.1865	$2.16 \times 10^{-2}$	311.16
6	0.1080	0.6108	1.5675	2.5179	3.1862	$4.02 \times 10^{-3}$	1064.55
MC+PSOR	0.1072	0.6119	1.5618	2.5233	3.1928		8388.97
MC Upper Bound	0.1097	0.6175	1.5688	2.5298	3.1988		
MC Lower Bound	0.1047	0.6063	1.55548	2.5168	3.1868		

TABLE 6. Mother prices (**American** put on **American** put) computed using the sparse grid (SG) with  $(c_1 = 16, c_2 = 8, c_3 = 4)$ . MC refers to the Longstaff & Schwartz (2001) with 1,000,000 sample paths, 500 time steps and 50 exercise dates. Parameter values are given in Table 1, with  $v_0 = 0.04$  and  $r_0 = 0.04$ .

exercise, we need to compare the continuation value and the immediate exercise payoff which is derived from the price of the daughter option at that particular time. However with the increase of the number of the time step of the mother option, the computational burden to workout the American daughter option prices at different time to maturity

will increase dramatically as well. Hence, a repeated Richardson extrapolation technique as described in Chang, Chung & Stapleton (2007) is used to find the prices of the compound option when the mother option is allowed to be exercised early. In this case, we are able to treat the mother option as a Bermudan option which can be exercised in a number of fixed time points before the maturity and here we use the geometric-spaced exercise points employed in the modified Geske-Johnson formula described in Chang et al. (2007). Table 6 shows the results of the Richardson extrapolation technique compared with the least squares Monte Carlo approach by Longstaff & Schwartz (2001) with the daughter option prices calculated from the PSOR with a very fine grid ( $N_1 = 1024, N_2 = 512, N_3 = 512, N_t = 128$ ). Boyarchenko & Levendorski (2007) and Medvedev & Scaillet (2010) have implemented the least squares Monte Carlo approach as a benchmark solution.

## 5. CONCLUSION

We have studied the pricing of American compound options by solving the corresponding PDE using both a sparse grid approach and a benchmark based on Monte Carlo Simulation together with the PSOR approach.

It turns out that application of the standard sparse grid (SG) approach is able to provide fairly accurate and efficient results for the compound option prices under Heston with stochastic interest rate. We apply this method twice to solve both PDEs followed by the price of the daughter option and the price of the mother option. We develop a benchmark solution by applying the finite difference with PSOR approach to solve the PDE followed by the daughter option in a fine grid. Then using these results to specify the appropriate boundary conditions, we employ least squares Monte Carlo simulation to find the prices of the mother option. The numerical results show clearly the computational advantage of the SG approach compared with the MC/PSOR approach.

In future research, the sparse grid approach can be speeded up by using better PDE solvers, such as the operator splitting in Ikonen & Toivanen (2004) and Ikonen & Toivanen (2007) with a modified adaptive sparse grid. The method may be applied to tackle specific examples in real options applications such as multi-stage investment projects, where it is important to take account of both stochastic volatility and stochastic interest rate due to the sensitivity of the compound options to volatility.

## REFERENCES

- Black, F. & Scholes, M. (1973), ‘The Pricing of Corporate Liabilities’, *Journal of Political Economy* **81**, 637–659.

- Boyarchenko, S. & Levendorski, S. (2007), American options in the Heston model with stochastic interest rate and its generalization. Available online at [http : //papers.ssrn.com/sol3/papers.cfm?abstract\\_id = 1031282](http://papers.ssrn.com/sol3/papers.cfm?abstract_id=1031282) >.
- Brenner, M., Ou, E. & Zhang, J. (2006), ‘Hedging Volatility Risk’, *Journal of Banking and Finance* **30**(3), 811–821.
- Chang, C.-C., Chung, S.-L. & Stapleton, R. (2007), ‘Richardson extrapolation techniques for the pricing of american-style options’, *The Journal of Futures Markets* **27**(8), 791–817.
- Chiarella, C., Ziogas, A. & Ziveyi, J. (2010), *Contemporary Quantitative Finance: Essays in Honour of Eckhard Platen*, Springer, chapter Representation of American Option Prices Under Heston Stochastic Volatility Dynamics Using Integral Transforms, pp. 281–315.
- Ekstrom, E., Lotstedt, P. & Tysk, J. (2009), ‘Boundary values and finite difference methods for the single factor term structure equation’, *Applied Mathematical Finance* **16**(3), 253–259.
- Fouque, J. P. & Han, C. H. (2005), ‘Evaluation of Compound Options Using Perturbation Approximation’, *Journal of Computational Finance* **9**(1), 41–61.
- Geske, R. (1979), ‘The Valuation of Compound Options’, *Journal of Financial Economics* **7**, 63–81.
- Geske, R. & Johnson, H. E. (1984), ‘The American Put Option Valued Analytically’, *Journal of Finance* **39**(5), 1511–1524.
- Griebel, M., Schneider, M. & Zenger, C. (1992), *A combination technique for the solution of sparse grid problems*, Elsevier, Amsterdam, chapter Iterative Methods in Linear Algebra, pp. 263–281.
- Grzelak, L. & Oosterlee, C. (2011), ‘On the heston model with stochastic interest rates’, *SIAM J. Financial Math.* **2**, 255–286.
- Han, C. H. (2003), *Singular Perturbation on Non-Smooth Boundary Problems in Finance*, Dissertation, North Carolina State University.
- Heston, S. (1993), ‘A Closed-Form Solution for Options with Stochastic Volatility with Applications to Bond and Currency Options’, *Review of Financial Studies* **6**(2), 327–343.
- Ikonen, S. & Toivanen, J. (2004), ‘Operator Splitting Methods for American Options with Stochastic Volatility’, *Applied Mathematics Letters* **17**, 809–814.
- Ikonen, S. & Toivanen, J. (2007), ‘Componentwise Splitting Methods for Pricing American Options under Stochastic Volatility’, *International Journal of Theoretical and Applied Finance* **10**(2), 331–361.
- Kodukula, P. & Papudesu, C. (2006), *Project Valuation Using Real Options: A Practitioner’s Guide*, J. Ross Publishing.
- Kwok, Y.-K. (2008), *Mathematical Models of Financial Derivatives*, 2nd edn, Springer.
- Leentvaar, C. & Oosterlee, C. (2008a), ‘Multi-asset option pricing using a parallel fourier-based technique’, *Journal of Computational Finance* **12**(1), 1–26.
- Leentvaar, C. & Oosterlee, C. (2008b), ‘On coordinate transformation and grid stretching for sparse grid pricing of basket options’, *Journal of Computational and Applied Mathematics* **222**, 193–209.
- Longstaff, F. & Schwartz, E. (2001), ‘Valuing american options by simulation: a simple least-squares approach’, *Review of Financial Studies* **14**, 113–147.
- Medvedev, A. & Scaillet, O. (2010), ‘Pricing American Options under Stochastic Volatility and Stochastic Interest Rates’, *Journal of Financial Economics* **98**, 145–159.
- Reisinger, C. (2004), *Numerische Methoden für hochdimensionale parabolische Gleichungen am Beispiel von Optionspreisaufgaben*, PhD thesis, Universität Heidelberg.
- Reisinger, C. (2008), *Analysis of Linear Difference Schemes in the Sparse Grid Combination Technique*, Technical report, Mathematical Institute, Oxford, UK.

Reisinger, C. & Wittum, G. (2007), 'Efficient Hierarchical Approximation of High-Dimensional Option Pricing Problems', *SIAM Journal on Scientific Computing* **29**(1), 440–458.